Indian Journal of Engineering & Materials Sciences
Vol. 27, April 2020, pp. 348-355

Influence of micro-structural parameters on fatigue life of discontinuous reinforced metal matrix composites

Abhishek Tevatia[a *] & Sunil Kumar Srivastava[b]

[a]Department of Mechanical Engineering, Netaji Subhas University of Technology, Dwarka, New Delhi – 110078, India

[b]Mechanical Engineering Department, Madan Mohan Malaviya University of Technology, Gorakhpur, Uttar Pradesh 273 010, India

Received: 17 September 2017 ; Accepted: 22 October 2018

The micro-structural parameters such as reinforcement shape, size, distribution, volume fraction, property mismatch, aging condition, bonding strength, and whisker orientation can influence the fatigue life of discontinuous reinforced metal matrix composites (DRMMCs). The strengthening effect plays a vital role in predicting the fatigue behaviour of DRMMCs. The modified shear lag (MSL) and enhance dislocation density (EDD) are two main factors that describes the strength of DRMMCs. In the present work, fatigue crack growth life model based MSL and EDD strengthening mechanism has been developed by integrating fatigue damage deformation at the crack-tip under the total strain-controlled conditions. The closed form expression predicts the dependency of particle size, reinforcement volume fraction and reinforcement constraint of the matrix on the fatigue crack growth life. The model fitting with experimental data affirms the appropriateness of proposed fatigue crack growth life prediction model for DRMMCs.

Keywords: Fatigue crack growth life, Enhance dislocation density, Fatigue damage zone, Micro-structural, Discontinuous reinforced metal matrix composites

1 Introduction

The fatigue is a complex metallurgical process in discontinuous reinforced metal matrix composites (DRMMCs). Fatigue results the cyclic/recurring variable stress levels within the material, the area around reinforcements, and the mismatch in stiffness of its constituents. The matrix in DRMMC could lock-in stresses during manufacturing or under the application of mechanical loading[1-3]. It has been established that the fatigue crack growth life of DRMMCs can be controlled by the micro-structural parameters such as particle size(alternatively, the aspect ratio), reinforcement volume fraction, interfacial bonding strength, constraints of particle in matrix material, *etc.* A well-established fatigue crack growth model can help in avoiding the catastrophic failure so that replacement can be done well in advance[4-7].

Over the last two decades, a few analytical fatigue life prediction models, based on the micro-structural features of DRMMCs, have been developed[8-13]. Bruzzi *et al.*[8]proposed the micromechanical model for predicting the fatigue life of Al-SiC DRMMC whereas Ding *et al.*[9-11]models are based up on the linear elastic fracture mechanics theory. The strengthening effect, attributed by the load bearing effect of hard reinforcement[14-16] and enhanced strength of matrix supported by the increase in dislocation density of matrix[17-20], plays an important role in the estimation of fatigue crack growth life. Many researchers[21-24]have used both the strengthening factors for predicting the strength of these composites. Ramakrishnan's[21]model is based on the strengthening factor that assumed increase in dislocation density due to increase in the residual plastic strain. Zhang *et al.*[25-26]developed a micro-structural based crack initiation model using the concept of Gibbs free energy[26]in which reinforcement size and yield strength is related to the fatigue life strengthened by both the modified shear lag(MSL) and enhanced dislocation density (EDD) of matrix[25].

In the present work, a closed form expression of fatigue crack growth life for DRMMCs based on the strengthening effect attributed by the load bearing effect of hard reinforcement (MSL model) and EDD of matrix is obtained. The proposed model can be used to study the influence of dislocation density of matrix for low cycle fatigue applications. The model predicts effects of the micro-structural parameters such as the reinforcement size, volume fraction, cyclic

*Corresponding author (E-mail: abhishek_tevatia@yahoo.co.in)

strain hardening exponent, cyclic strength coefficient and level of constraint in the crack-tip region on the fatigue crack growth life. The analytical results are compared with the experimental observations available in literature.

2 Fatigue Life Prediction Model

The concept of cyclic plastic zone (CPZ) in metals can be extended for the calculation of fatigue crack growth life of DRMMCs[9-13].It has been established that the prominent factors responsible for the actual degradation process are the enhanced dislocation density near the interface, the hydrostatic stresses within the constrained matrix, the brittle nature of fibres, the stress concentration and the plastic flow constraint of the metallic matrix due to the presence of reinforcement fibres[11,26].The micro-structural effect of reinforcement on the cyclic plastic deformation very near to the crack-tip, where the actual degradation occurs within the fatigue damage zone (FDZ), is considered in the present model.

2.1 Reinforcement strengthening mechanism

DRMMCs can be strengthened by the load bearing effect of hard reinforcement (MSL model)[14-16] and enhancement in the dislocation density of matrix (EDD model)[17-20]. The present model incorporates both the strengthening factors for estimating the fatigue crack growth life. The yield strength of DRMMCs based on the MSL and EDD models may be expressed as[21]

$$\sigma_{cy} = \sigma_{my}(1 + f_{MSL})(1 + f_{EDD}) \quad \ldots(1)$$

where, σ_{cy} is the cyclic yield strength of DRMMCs, σ_{my} the cyclic yield strength of matrix, f_{MSL} and f_{EDD} are the improvement factors quantifying the load bearing effect of hard reinforcement and dislocation strengthening of matrix, respectively.

The load bearing factor can also be calculated using MSL model[27] by considering the stress concentration at the particle end and stress behaviour of matrix from elastic to plastic state. The particle stress in plastic region relates the yield strength of DRMMCs with the yield strength of matrix alloy as[27]

$$\sigma_{cy} = \sigma_{my}\left[1 + \frac{8V_f{}^2(l/d)^2(E_f - E_m)}{3(E_f + 4V_f(l/d)^2E_m)}\right] \quad \ldots(2)$$

where, V_f the particle volume fraction, s the aspect ratio, E_m and E_f are modulus of elasticity of matrix and reinforcement materials, respectively.

For MSL model, the Eq. (1) can be rewritten as[21]

$$\sigma_{cy} = \sigma_{my}(1 + f_{MSL}) \quad \ldots(3)$$

Thus, Eqs. (2) & (3) gives load bearing factor as

$$f_{MSL} = \frac{8V_f{}^2(l/d)^2(E_f - E_m)}{3(E_f + 4V_f(l/d)^2E_m)} \quad \ldots(4)$$

The dislocation density factor, effective strain arising due to the residual thermal stresses, is expressed as[21]

$$f_{EDD} = \frac{kG_m b\sqrt{\rho}}{\sigma_{my}} \quad \ldots(5)$$

where, k the constant, G_m the shear modulus, b the Burger's vector and ρ the enhance dislocation density of matrix material.

The dislocation density for cube-shaped particle/fiber is given as[21]

$$\rho = \frac{12\Delta\alpha\Delta T V_f}{bd} \quad \ldots(6)$$

where, d the particle size, $\Delta\alpha$ the difference in coefficient of thermal expansions and ΔT the temperature difference. Thus, yield strength of composite may be expressed as

$$\sigma_{cy} = \sigma_{my}\left[\left(1 + \frac{8V_f^2(l/d)^2(E_f - E_m)}{3(E_f + 4V_f(l/d)^2E_m)}\right)\left(1 + \frac{3.464kG_m\sqrt{b\Delta\alpha\Delta TV_f}}{\sigma_{my}\sqrt{d}}\right)\right] \quad \ldots(7)$$

2.2 Crack-tip deformation characteristics for fatigue crack growth

The present model considers potential energy that is approximately equal to interaction energy between the stress-strain field and FDZ size. The J integral (local driving force) for non-linear material, the rate of change of potential energy with the crack advancement[28], is expressed as:

$$\Delta J = -\frac{\partial U_{int}}{\partial w_{FDZ,C}} \quad \ldots(8)$$

The interaction energy[29] for FDZ volume is given by:

$$U_{int} = -\int_u \bar{\sigma}\,\overline{\varepsilon_{pl}}\,du \quad \ldots(9)$$

where, $\bar{\sigma}$ the local cycle stress amplitude and $\overline{\varepsilon_{pl}}$ the accumulated average plastic strain.

The interaction energy can be used for the calculation of FDZ size by assuming the uniform local cyclic stresses equal to the matrix ultimate stress (σ_{mu})as:

$$U_{int} = -A_{FDZ}\sigma_{mu}\overline{\varepsilon_{pl}} = -\pi\sigma_{mu}\overline{\varepsilon_{pl}}\left(\frac{w_{FDZ,C}}{2}\right)^2 \quad \ldots(10)$$

where, $A_{FDZ} = \pi\left(\frac{w_{FDZ,C}}{2}\right)^2$ the area of FDZ and $w_{FDZ,C}$ the size of FDZ in DRMMC. The interaction energy per unit size is in the perpendicular direction to the crack-plane.

The accumulated plastic strain in FDZ may be expressed as:

$$\overline{\varepsilon_{pl}} = \frac{1}{W_{FDZ,C}}\int_0^{W_{FDZ,C}} \varepsilon_{pl}(w)dw \quad \ldots(11)$$

The stress-strain expressions within the CPZ without losing its generality may be written as[30]:

$$\frac{\sigma(w)}{2} = \frac{\Delta\sigma}{2}\left(\frac{W_{CPZ,C}}{w}\right)^{\frac{n'}{n'+1}} \quad \ldots(12)$$

$$\frac{\varepsilon_{pl}(w)}{2} = \frac{\Delta\varepsilon_{pl}}{2}\left(\frac{W_{CPZ,C}}{w}\right)^{\frac{1}{n'+1}} \quad \ldots(13)$$

where, $\frac{\Delta\sigma}{2}$thecyclic-plastic stress amplitude, $\frac{\Delta\varepsilon_{pl}}{2}$the cyclic-plastic strain amplitude and n' the cyclic strain hardening exponent.

The well-established concept of CPZ is used to evaluate the crack driving force. The CPZ includes FDZ very near to the crack-tip shown in Fig. 1. The local shearing takes place in FDZ during crack growth and the local cyclic stress level approaches to the ultimate tensile strength of DRMMCs[31-32]. The CPZ size, obtained from the elastic plastic fracture mechanics (EPFM) concept, may be expressed as[11,12,30,33]

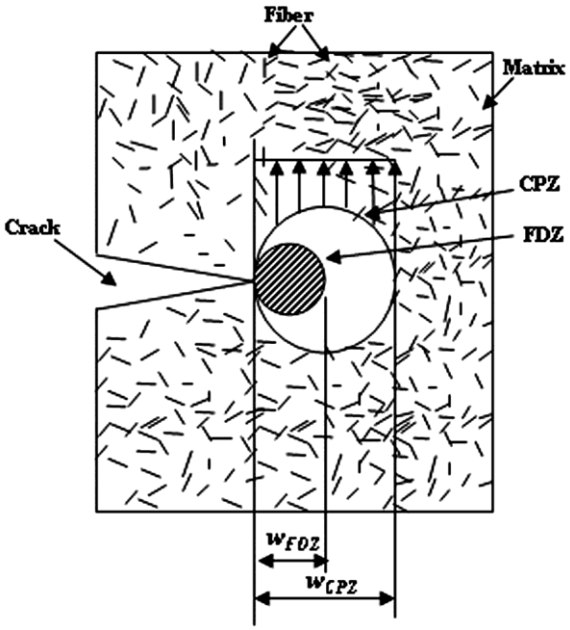

Fig. 1 — The fatigue crack-tip region including the cyclic plastic zone and the fatigue damage zone in DRMMC[13].

$$w_{CPZ,C} = \lambda_l\left(\frac{\Delta K_{eff}}{2\sigma_{my}}\right)^2 = \frac{\lambda_l Y^2\pi a}{4{C_\varepsilon}^2}\left(\frac{K'}{\sigma_{my}}\right)^2\left(\frac{\Delta\varepsilon_{pl}}{2}\right)^{2n'} \quad \ldots(14)$$

where, λ_l the correction factor under large-scale yielding (LSY), the effective stress intensity range based on cyclic stress-strain curve relationship $\Delta K_{eff} = \frac{\Delta\sigma_{eff}}{2}Y\sqrt{\pi a}$ in which the effective stress amplitude $\frac{\Delta\sigma_{eff}}{2} = \frac{1}{2C_\varepsilon}\frac{\Delta\sigma}{2}$ and $\frac{\Delta\sigma}{2} = K'\left(\frac{\Delta\varepsilon_{pl}}{2}\right)^{n'}$, Y the crack geometry correction factor, C_ε the constraint, K' the cyclic strength coefficient and a the crack length.

When $\frac{\Delta\sigma}{2}$ approaches the σ_{mu} (ultimate tensile strength), the size of FDZ (Eq. 12) may be expressed as

$$w_{FDZ,C} = w_{CPZ,C}\left(\frac{\Delta\sigma}{2\sigma_{mu}}\right)^{\frac{n'+1}{n'}} = \frac{\lambda_l Y^2\pi a}{16{C_\varepsilon}^2}\left(K'^{(3n'+1/n')}/{\sigma_{my}}^2{\sigma_{mu}}^{n'+1/n'}\right)\left(\frac{\Delta\varepsilon_{pl}}{2}\right)^{3n'+1} \quad \ldots(15)$$

and, incorporating the micro-structural and strengthening effects gives

$$w_{FDZ,C} = \frac{\lambda_l Y^2\pi a}{16{C_\varepsilon}^2}\left[\left(1+\frac{8{V_f}^2(l/d)^2(E_f-E_m)}{3(E_f+4V_f(l/d)^2E_m)}\right).\left(1+\frac{3.464kG_m\sqrt{b\Delta\alpha\Delta TV_f}}{\sigma_{my}\sqrt{d}}\right)\right]^2 \left(K'^{(3n'+1/n')}/{\sigma_{cy}}^2{\sigma_{mu}}^{n'+1/n'}\right)\left(\frac{\Delta\varepsilon_{pl}}{2}\right)^{3n'+1} \quad \ldots(16)$$

The accumulated average plastic strain ($\overline{\varepsilon_{pl}}$), calculated from Eqs. (11 & 13), may be substituted in Eq. (10) to find out the interaction energy as

$$U_{int} = -\pi\left(\frac{n'+1}{n'}\right)\sigma_{mu}^{\frac{n'+1}{n'}}\left(\frac{1}{K'}\right)^{\frac{1}{n'}}\left(\frac{w_{FDZ,C}}{2}\right)^2 \quad \ldots(17)$$

The cyclic J integral, required to propagate the crack, may be obtained by integrating Eq. (17) as

$$\Delta J = \frac{\lambda_l Y^2\pi^2 a}{32{C_\varepsilon}^2}\left[\left(1+\frac{8{V_f}^2(l/d)^2(E_f-E_m)}{3(E_f+4V_f(l/d)^2E_m)}\right)\left(1+\frac{3.464kG_m\sqrt{b\Delta\alpha\Delta TV_f}}{\sigma_{my}\sqrt{d}}\right)\right]^2\left(\frac{n'+1}{n'}\right)\left(\frac{K'^3}{{\sigma_{cy}}^2}\right)\left(\frac{\Delta\varepsilon_{pl}}{2}\right)^{3n'+1} \quad \ldots(18)$$

2.3 Fatigue crack growth life

The cyclic J integral correlates the crack-tip opening displacement (CTOD) as[34]

$$\Delta J = \omega \sigma_{cy} \Delta CTOD \quad \ldots(19)$$

where, ω is taken 1 for the plane stress and 2 for the plane strain conditions. The $\Delta CTOD$ for plain strain condition may be expressed as:

$$\Delta CTOD = \frac{\lambda_l Y^2 \pi^2 a}{64 C_\varepsilon^{\,2}} \left[\left(1 + \frac{8 V_f^{\,2} (l/d)^2 (E_f - E_m)}{3(E_f + 4 V_f (l/d)^2 E_m)} \right) \left(1 + 3.464 k G_m b \Delta a \Delta TV f \sigma_{my} d 2n' + 1 n' K' \sigma_{cy} 3 \Delta \varepsilon_{pl} 23n' + 1 \right.$$

...(20)

The fatigue crack growth rate, equal to one-half of the CTOD[31], is expressed as

$$\frac{da}{dN} = \frac{\lambda_l Y^2 \pi^2 a}{128 C_\varepsilon^{\,2}} \left[\left(1 + \frac{8 V_f^{\,2} (l/d)^2 (E_f - E_m)}{3(E_f + 4 V_f (l/d)^2 E_m)} \right) . \left(1 + 3.464 k G_m b \Delta a \Delta TV f \sigma_{my} d 2n' + 1 n' K' \sigma_{cy} 3 \Delta \varepsilon_{pl} 23n' + 1 \right.$$

...(21)

The fatigue crack growth life, incorporating both the load bearing effect and dislocation density effect, may be calculated by integrating Eq. (21) from the initial crack length (a_i) to the fracture length (a_f)may be expressed as:

$$2N_f = \frac{256 C_\varepsilon^{\,2}}{\lambda_l Y^2 \pi^2} \left[\left(1 + \frac{8 V_f^2 (l/d)^2 (E_f - E_m)}{3(E_f + 4 V_f (l/d)^2 E_m)} \right) \left(1 + \frac{3.464 k G_m \sqrt{b \Delta \alpha \Delta TV_f}}{\sigma_{my} \sqrt{d}} \right) \right]^{-2} . \left(\frac{n'}{n'+1} \right) \left(\frac{\sigma_{cy}}{K'} \right)^3 ln \left(\frac{a_f}{a_i} \right) \left(\frac{\Delta \varepsilon_{pl}}{2} \right)^{-(3n'+1)} \quad \ldots(22)$$

3 Results

Table 1 lists the parameters used in the calculation of fatigue crack growth life for different DRMMCs. For aluminum based DRMMCs, $C_\varepsilon = 0.2$ and $Y = 1.12$[35,36], b = 2.86×10^{-10} m and k = 1.25 are used[21,26,35,36]. Moreover, initial crack size a_i =5 μm and final critical crack length a_f = 2 mm are considered for the high strength aluminium alloy[37,38]. The increment in dislocation density starts around 800 K; thus, ΔT = 510 K is considered[11,38]. Using one of the experimental values of $\frac{\Delta \varepsilon_{pl}}{2}$ the λ_l can be calculated as[33]:

$$\lambda_l = \frac{\pi}{18} \left(\frac{1}{2} + \frac{2}{3} \sqrt{\frac{2}{3}} \frac{\Delta \sigma_{eff}}{2 \sigma_{cy}} \right) \quad \ldots(23)$$

Table 1 — Mechanical parameters of aluminum based DRMMCs.

DRMMCs / Parameter	AA2014-$Al_2O_{3(P)}$ tested at 100 °C[39,43-44]	AA6061-$Al_2O_{3(P)}$ tested at 25°C[11, 43-44]	AA6061 (D20)-$Al_2O_{3(P)}$ tested at Room Temp.[40,43-44]	AA6061(C85) -$Al_2O_{3(P)}$ tested at Room Temp.[40,43-44]
E_c(GPa)	89	93.3	92.6	89
E_m(GPa)	72	71	71	71
E_f(GPa)	312	312	312	312
G_m(GPa)	28	26	26	26
n'	0.14	0.16	0.15	0.14
K'(MPa)	580	1066	869	824
σ_{cy}(MPa)	467	387	398	389
σ_{my}(MPa)	414	340	368	352
V_f	0.15	0.15	0.2	0.2
λ_l	0.1885	0.3497	0.2565	0.2635
α_m (10^{-6}/°C)	23.6	24.3	23.2	23.8
α_f (10^{-6}/°C)	7.4	7.4	7.4	7.4

3.1 Relevancy of present model

Figure 2 predict the fatigue crack growth lives for different DRMMCs (Eq. 22), incorporating the load bearing effect of hard reinforcement (MSL model) and dislocation density of matrix (EDD model), shows good agreement with the experimental data available in literature[11,39,40].

3.2 Influence of micro-structural parameters on the fatigue crack growth life

The influence of micro-structural parameters such as reinforcement size, reinforcement volume fraction and the level of constraint near the crack-tip on the fatigue crack growth life of AA2014- $Al_2O_{3(P)}$ DRMMC (at 100 °C[39]) are investigated. By considering four different experimental $\frac{\Delta \varepsilon_{pl}}{2}$, *viz.*, 4.81×10^{-4}, 3.58×10^{-4}, 2.02×10^{-4} and 1.89×10^{-4}, all under total strain controlled condition[39]. Figure 3 shows the effect of reinforcement size (d) (assuming cubic particle; alternatively, unity aspect ratio) on the fatigue crack growth life ($2N_f$) of AA2014- $Al_2O_{3(P)}$ DRMMC, keeping plastic strain amplitude $\left(\frac{\Delta \varepsilon_{pl}}{2}\right)$as a parameter. For the entire range of d, higher level $\frac{\Delta \varepsilon_{pl}}{2}$ results into lower $2N_f$. For a given $\frac{\Delta \varepsilon_{pl}}{2}$ level, initially the $2N_f$ decreases rapidly (up to 5 μm), followed by gradual decrease with an increase in the d. Higher d results into earlier crack growth; consequently, leads to a lower $2N_f$ when $\frac{\Delta \varepsilon_{pl}}{2}$ is kept constant. Chawla *et al.*[38] and Bosi *et al.*[41] observed the similar results for AA2080-SiC and AA6061-Al_2O_3 particle reinforced composites, respectively.

Figure 4 shows the effect of volume fraction(V_f) on the $2N_f$ keeping $\frac{\Delta \varepsilon_{pl}}{2}$ as a parameter. A high $\frac{\Delta \varepsilon_{pl}}{2}$ results into earlier crack growth; consequently, leads to low $2N_f$ which has been experimentally[40]

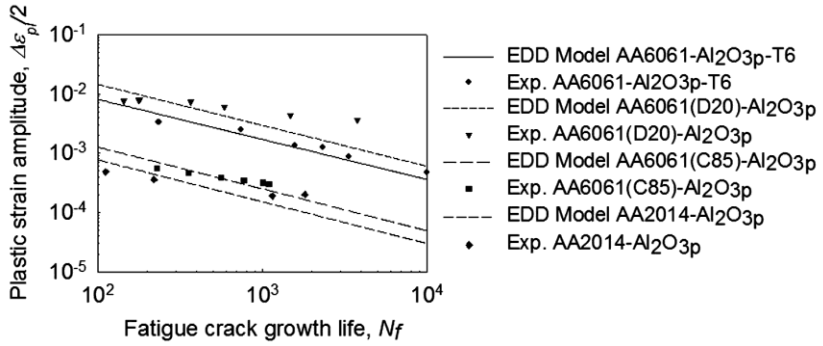

Fig. 2 — Enhanced dislocation density-based crack propagation fatigue life model for different DRMMCs AA6061-Al_2O_{3p}-T6 tested at 25 °C, d = 15μm; AA6061(D20)-Al_2O_{3p} tested at room temperature, d = 12.6μm; AA6061(C85)-Al_2O_{3p} tested at room temperature, d = 12.6 μm and AA2014-Al_2O_{3p} tested at 100 °C, d = 15 μm.

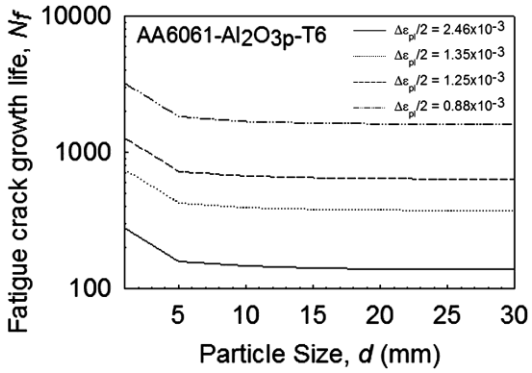

Fig. 3 — Effect of particle size on fatigue crack growth life of AA2014-Al_2O_3 DRMMC

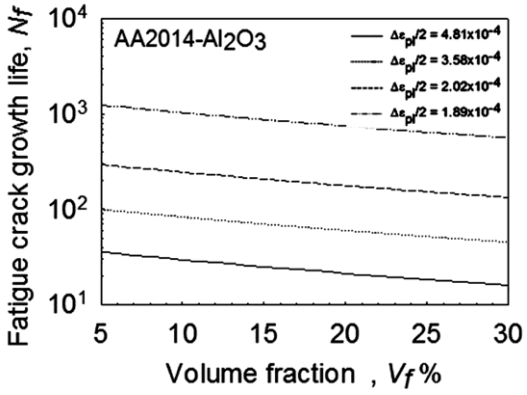

Fig. 4 — Effect of reinforcement volume fraction on the fatigue crack growth life of AA2014-Al_2O_3 DRMMC

validated. Higher V_f leads to low fatigue strength of composite[4,9]. For given $\frac{\Delta\varepsilon_{pl}}{2}$, the LCF strength of DRMMCs is normally inferior to that of the unforced matrix if compared in terms of $\frac{\Delta\varepsilon_{pl}}{2}$ (either total or elastic)[4, 9-11]. For given $\frac{\Delta\varepsilon_{pl}}{2}$, it has been established that the $2N_f$ of DRMMCs decreases at least one order of magnitude with an increase in the V_f of composite [9-11].

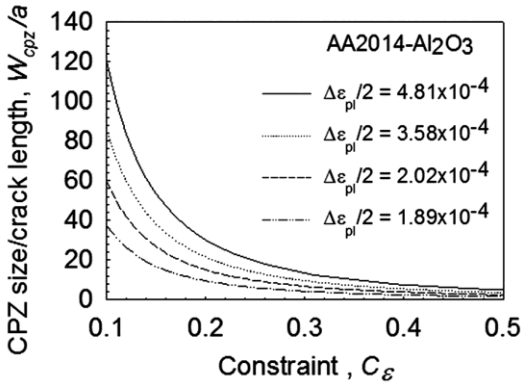

Fig. 5 — Effect of constraint on the CPZ size per unit crack length forAA2014-Al_2O_3 DRMMC

The constraint 'C_ε' (*viz.*, ratio of mean to effective strain/stress)is defined by the level of proximity of crack-tip to the reinforced discontinuous particles/fibres. The actual degradation occurs in the CPZ ahead of the crack-tip during fatigue crack propagation and the C_ε affects the CPZ size'$w_{CPZ,C}$'. Figure 5 shows the effect of constraint on the $w_{CPZ,C}$ for different level of $\frac{\Delta\varepsilon_{pl}}{2}$. For entire range of C_ε (0 to 0.5), the higher $\frac{\Delta\varepsilon_{pl}}{2}$results into large $w_{CPZ,C}$ whereas the lower C_ε results into large $w_{CPZ,C}$. These observations support the statement "*constraint is high when the fatigue crack-tip plastic zone is small"*[35].

3.3 Sensitivity of fatigue crack growth life

The fatigue crack growth life is directly proportional to $[ln(a_f/a_i)]$. Figures 6 and 7, respectively, shows the fatigue crack growth life of AA6061-Al_2O_{3p}-T6 DRMMC with initial crack length (a_i) and fracture crack length (a_f) as a parameter, respectively. The sensitivity of present model is

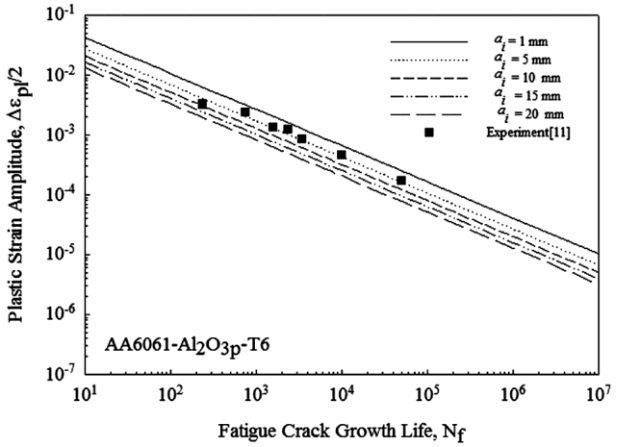

Fig. 6 — Fatigue crack growth life of AA6061-Al_2O_{3p}-T6 DRMMC with initial crack length as a parameter.

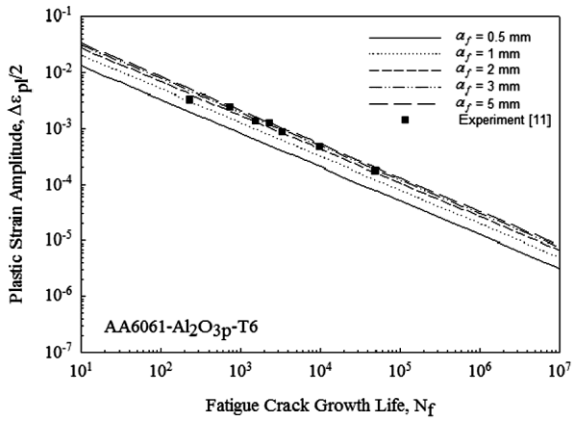

Fig. 7 — Fatigue crack growth life of AA6061-Al_2O_{3p}-T6 DRMMC with fracture crack length as a parameter.

investigated for the aluminum based DRMMC by assuming a_i = 5 μm (Fig. 6) and a_f = 2 mm (Fig. 7). For $(\Delta\varepsilon_{Pl}/2)$= 2.41×10^{-3}, the fatigue life increases by 20% when initial crack length (a_i) decreases to 1 μm (Fig. 6); however, it decreases by 13% when crack length (a_i) increases up to 15 μm. Similarly, for $(\Delta\varepsilon_{Pl}/2)$= 2.41×10^{-3}, the fatigue life decreases by 10% if fracture crack length (a_f) reduces up to 0.5 mm and increases by 12% when crack length (a_f) increases up to 5 mm (Fig. 7).

4 Discussion

The aim of present work is to model the deformation field near the crack-tip and cyclic plastic flow behavior for better understanding of effects of micro-structural parameters. The model, based on the physical significance of fatigue damage, considers the constraint of fiber/particle on the matrix plasticity. It is evident from the closed form expression that under the total strain controlled conditions, both the local driving force in FDZ very near to crack-tip (Eq. 18) and the crack growth rate (Eq. 21) is directly correlated with the range of crack-tip opening displacement ($\Delta CTOD$). The analytical results (Fig. 2) are found to be in good agreement with the experimental observations over the wide range of plastic strain amplitudes.

The mechanical aspect and micro-structural features such as the reinforcement size, the volume fraction, the constraint level near the crack-tip and the interfacial strength are considered in the fatigue crack growth propagation. The modeling is based on the fatigue damage evolution of the micro-structural element within the FDZ and fatigue behavior is treated as localized damage. The fatigue crack growth process within the FDZ is dominated by the localized cyclic stress, the stress concentration and micro-structural fatigue damage evolution. When stresses generated exceeds the ultimate tensile strength, the propagation of micro-crack stops if local cyclic stress level reduces to $\Delta\sigma/2 = \sigma_{my}$.

Strengthening mechanics is one of the important aspect in the evaluation of fatigue crack growth life. In DRMMCs, strengthening effects is attributed by the load bearing effect of hard reinforcement (MSL model) and the dislocation density of matrix (EDD model). Moreover, the dislocation density influences the reinforcement size, not the volume fraction. Figure 3 depicts the decrease in fatigue crack growth life with an increase in the particle size. The yield strength (367.89MPa) for AA6061-Al_2O_{3P}-T6 DRMMC obtained analytically (Eq.7) is comparable with the experimental observation (387 MPa). The finite element analysis[42]showsthat short-crack trapping depends upon the reinforcement size and the volume fraction; moreover, finer particles possess better fatigue strength for a given volume fraction of composite (Fig. 1). It should be noted that dislocation barriers play a vital role in the process of crack growth. The reinforcement poses strong barrier to dislocation movement and area surrounded by the particle experiences high internal multi-axial stresses.

In the present work, $\Delta CTOD$ is used as a correlating parameter to show the dependency of fatigue crack growth on the mechanical aspects and the micro-structural features of DRMMCs. The opening of crack near the tip controls the material deformation; hence, it is sensible to assume that $\Delta CTOD$ is directly related to the kinetics of fatigue

crack growth. This concept can be used to explain the fatigue crack growth rate dependency on the elastic modulus for the wide range of metals. The experimental measurement of $\Delta CTOD$ in DRMMC is very difficult and time consuming; hence, fatigue crack growth model must include the parameters such as the crack length, the volume fraction, the applied plastic strain amplitude and the yield strength of material.

The CPZ correction factor (λ_l) is another important parameter that depends upon the material behavior, sample thickness, yielding criteria (whether small-scale or large-scale yielding) and independent tothe temperature. The magnitude of correction factor for DRMMCs is higher compared with the unreinforced metal due to the influence of micro-structural parameters such as aspect ratio, reinforcement size, and the volume fraction of reinforcements. The local mix-mode loading near the crack when the location of crack is very close to the interface, may change the CPZ size, the effective driving force, the crack growth rate and microscopic damage, *etc.*[37].

The fatigue damage evolution is complex in DRMMCs than the pure metals[4-11].The uniqueness of presented model is to incorporate the physical process of fatigue damage evolution in which the micro-structural parameters establisha relationship between the microscopic and the macroscopic processes under the total strain conditions.

5 Conclusions

The closed form expression, incorporating both the strengthening effects attributed by the load bearing effect of hard reinforcement (MSL model) and enhanced dislocation density of matrix(EDD model) as well as constraint in the matrix, is obtained to estimate the fatigue crack growth life of DRMMCs, and to investigate the influence of dislocation density in low cycle fatigue applications. The present model can predict the dependency of particle size on the fatigue crack growth life and connects MSL factor with volume fraction in a well-defined manner. The following conclusions are drawn based on the analytical results:

(i) The cyclic plastic deformation in the crack-tip is the main principal mechanical driving force for the propagation of fatigue crack under the fully strain controlled condition.

(ii) The reduction in reinforcement size results into higher fatigue crack growth life.

(iii) The analytical fatigue crack growth model based on MSL theory and EDD of matrix shows excellent agreement with the available experimental observations.

Nomenclature

a	crack length
A_{FDZ}	area of FDZ
b	Burgers vector of the matrix
C_ε	constraint
d	particle size
E	modulus of elasticity
E_m	modulus of elasticity of matrix material
E_f	modulus of elasticity of reinforcement material
f_{MSL}	improvement factor related MSL
f_{EDD}	improvement factor related to EDD
G_m	shear modulus of the matrix material.
G_{mc}	strain energy rate required to propagate the micro-crack
s	particle aspect ratio
k	material constant
U_{int}	interaction energy
V_f	reinforcement volume fraction
$w_{CPZ,C}$	cyclic plastic zone size for DRMMCs
$w_{FDZ,C}$	FDZ size for DRMMCs
σ_{cy}	cyclic yield strength of DRMMCs
σ_{my}	cyclic yielding strength of matrix
Y	crack geometry correction factor
$\Delta\alpha$	difference in the coefficient of thermal expansion
ΔT	temperature difference
$\frac{\Delta\sigma}{2}$	cyclic-plastic stress amplitude
$\frac{\Delta\varepsilon_{pl}}{2}$	cyclic-plastic strain amplitude
$\frac{\Delta K_{eff}}{2}$	effective stress intensity range
$\frac{\Delta\sigma_{eff}}{2}$	effective stress amplitude
$\overline{\varepsilon_{pl}}$	accumulated average plastic strain
K'	cyclic strength coefficient
λ_l	correction factor under the large-scale yielding
n'	cyclic strain hardening exponent
ρ	enhance dislocation density
$\bar{\sigma}$	local cycle stress amplitude
ν	Poisson's ratio

References

1 Kainer U K, *Metal matrix composite custom-made materials for automotive and aerospace engineering*, (Wiley-VCH, Germany), 2006.
2 Surappa M K, *Sadhana*, 28 (2003) 319.
3 Clyne T W & Withers P, *An introduction to metal matrix composites*, (Cambridge University Press, Cambridge), 1992.
4 Llorca J, *Prog Mater Sci*, 47 (2002) 283.
5 Hurd NJ, *Mater Sci Technol*, 4 (1988) 513.
6 Shang JK& Ritchie R O, In: *Metal matrix composites: mechanisms and properties*, (Academic Press, Boston) 1991, 255.
7 Hartmann O, Kemnitzer M & Biermann H, *Int J Fatigue*, 24 (2002) 215.
8 Bruzzi M S &McHugh P E, *Int J Fatigue*, 26 (2004) 795.
9 Ding H-Z, Biermann H & Hartmann O, *Compos Sci Technol*, 62 (2002) 2189.
10 Ding H-Z, Hartmann O, Biermann H & Mughrabi H, *Mater Sci Eng A*, 333 (2002) 295.
11 Ding H-Z, Biermann H & Hartmann O,*Int J Fatigue*, 25 (2003) 209.
12 Tevatia A & Srivastava S K, *Int J Fatigue*,70 (2015) 123.
13 Tevatia A& Srivastava S K, *Fatigue Fract Eng Mater Struct*, 40 (2017) 81.
14 Nardone V C and Prewo K M, *Scr Metall*, 20 (1986) 43.
15 Nardone V C, *Scripta Metall*, 21 (1987) 1313.
16 Piggot M R, *Load-Bearing Fibre Composites*,(Pergamon Press, Oxford), 1980.
17 Vogelsang M, Arsenault R H &Fisher R M, *Metall Trans*, 17 (1986) 379.
18 Arsenault R J & Shi N, *Mater Sci Eng*, 81 (1986) 175.
19 Arsenault R J, Wang L & Feng C R, *Acta Metall Mater*, 39 (1991) 47.
20 Shi N, Wilner B & Arsenault R J, *Acta MetallMater*, 40 (1992) 2841.
21 Ramakrishnan N, *Acta Mater*, 44 (1996) 69.
22 Wu Y, Lavernia E J, *Scr Metall*, 27 (1992)173.
23 Pickard S M, Schmauder S, Zahl D B &Evans A G, *Acta Metall Mater*, 40 (1992) 3113.
24 Hirth J P, *Scr Metall*, 25 (1991) 1.
25 Zhang Q & Chen D L, *ScrMater*, 51 (2004) 863.
26 Zhang Q &Chen D L,*Int J of Fatigue*, 27 (2005) 417.
27 Jiang Z, Lian J, Yang D & Dong SJ,*Mater Sci Tech*, 14 (1998) 517.
28 Rice J R, *J Appl Mech*, 35 (1968) 379.
29 Eshelby J D, *Proc R Soc A*, 241 (1957) 376.
30 Rice J R,In: *Fatigue Crack Propagation*, (ASTM STP 415, ASTM, PA) 1967, 247.
31 Tomkins B, *Philos Mag*, 18 (1968)1041.
32 Yong J O & Soo W N, *J Mater Sci*, 27 (1992) 2019.
33 Lu T J & Chow C L, *Eng Fract Mech*, 37(1990) 551.
34 Broek D, *Elementary engineering fracture mechanics* (The Netherlands: Sijthoff & Noordhoff), 1978.
35 Davidson D L & McClung R C, *Int J Fract*, 84 (1997) 81.
36 Laird C, In: *Fatigue Crack Propagation* (ASTM STP 415, ASTM, PA), 1967, 131.
37 Levin M & Karlsson B, *Int J Fatigue*, 15 (1993) 377.
38 Chawla N, Andres C, Jones J W & Allison J E, *Indust Heat*, (1999) 61.
39 Srivatsan T S, *Int J Fatigue*, 17 (1995) 183.
40 Hadianfard M J & Mai Y W, *J Mater Sci*, 31 (2000) 1715.
41 Bosi C, Garagnani G L, Tovo R & Vedani M, *Int J Mater Prod Technol*, 17 (2002) 228.
42 Li Chingshen & Ellyin F,*Compos Sci Technol*, 52 (1994)117.
43 *Metals Handbook, Vol.2 - Properties and Selection: Nonferrous Alloys and Special-Purpose Materials* (ASM International 10thEd.), 1990.
44 *Technical Report-18,Coefficient of Thermal Expansion for Various Materials at Different Temperatures* (Bal Seal Engineering), 2004.